CXCR3-dependent accumulation and activation of perivascular macrophages is necessary for homeostatic arterial remodeling to hemodynamic stresses

Jing Zhou,[1] Paul C.Y. Tang,[1] Lingfeng Qin,[1] Peter M. Gayed,[2] Wei Li,[1] Eleni A. Skokos,[3] Themis R. Kyriakides,[3] Jordan S. Pober,[2,3] and George Tellides[1,4]

[1]Department of Surgery, [2]Department of Immunobiology, and [3]Department of Pathology, Interdepartmental Program in Vascular Biology and Therapeutics, Yale University School of Medicine, New Haven, CT 06510
[4]Veterans Affairs Connecticut Healthcare System, West Haven, CT 06516

Sustained changes in blood flow modulate the size of conduit arteries through structural alterations of the vessel wall that are dependent on the transient accumulation and activation of perivascular macrophages. The leukocytic infiltrate appears to be confined to the adventitia, is responsible for medial remodeling, and resolves once hemodynamic stresses have normalized without obvious intimal changes. We report that inward remodeling of the mouse common carotid artery after ligation of the ipsilateral external carotid artery is dependent on the chemokine receptor CXCR3. Wild-type myeloid cells restored flow-mediated vascular remodeling in CXCR3-deficient recipients, adventitia-infiltrating macrophages of Gr1^{low} resident phenotype expressed CXCR3, the perivascular accumulation of macrophages was dependent on CXCR3 signaling, and the CXCR3 ligand IP-10 was sufficient to recruit monocytes to the adventitia. CXCR3 also contributed to selective features of macrophage activation required for extracellular matrix turnover, such as production of the transglutaminase factor XIII A subunit. Human adventitial macrophages displaying a CD14$^+$/CD16$^+$ resident phenotype, but not circulating monocytes, expressed CXCR3, and such cells were more frequent at sites of disturbed flow. Our observations reveal a CXCR3-dependent accumulation and activation of perivascular macrophages as a necessary step in homeostatic arterial remodeling triggered by hemodynamic stress in mice and possibly in humans as well.

CORRESPONDENCE
George Tellides:
george.tellides@yale.edu.

Abbreviations used: FXIIIA, factor XIII A subunit; iNOS, inducible nitric oxide synthase; Mig, monokine induced by IFN-γ; MMP, matrix metalloproteinase; MyD88, myeloid differentiation protein 88; TGM2, transglutaminase 2.

Hemodynamic forces modulate the size and thickness of blood vessels through structural alterations of the vessel wall termed vascular remodeling (Langille, 1996). Increased blood flow leads to vessel enlargement, whereas decreased blood flow leads to vessel shrinkage (Kamiya and Togawa, 1980; Langille et al., 1989). Proportional changes in medial mass under these circumstances keep wall thickness constant. In contrast, increased blood pressure results in thickened vessel walls (Baumbach and Heistad, 1989). These adaptive responses of the vessel wall to hemodynamic stresses are critical in arterial development and growth as well as in arterial disease (Hong et al., 2002; le Noble et al., 2004). The process of vascular remodeling requires reorganization of the cellular and extracellular matrix components of the vessel wall. Cellular turnover involves smooth muscle cell proliferation, apoptosis, and migration (Rudic et al., 1998, 2000; Korshunov and Berk, 2003). In addition, extracellular matrix turnover depends on degradation by proteinase enzymes, e.g., matrix metalloproteinases (MMPs), synthesis by smooth muscle cells, and cross-linking by enzymes with transglutaminase activity, such as transglutaminase 2 (TGM2) and factor XIII A subunit (FXIIIA; Bassiouny et al., 1998; Galis et al., 2002; Bakker et al., 2006).

The Rockefeller University Press $30.00
J. Exp. Med. Vol. 207 No. 9 1951-1966
www.jem.org/cgi/doi/10.1084/jem.20100098

The Journal of Experimental Medicine

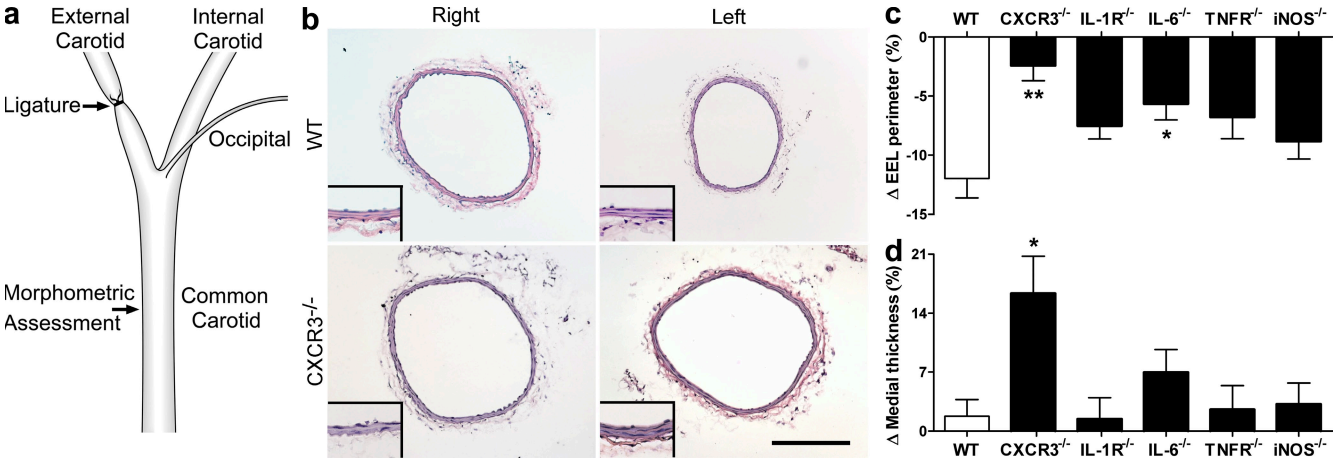

Figure 1. CXCR3 is necessary for flow-mediated inward vascular remodeling. (a) The left external carotid artery was ligated, and morphometric assessment at the midpoint of the left and right common carotid arteries was performed after 2 wk. (b) Representative photomicrographs of hematoxylin and eosin–stained transverse sections of right (unligated side) and left (ligated side) common carotid arteries in WT and CXCR3$^{-/-}$ mice. Bar, 200 µm. The vessel walls at twofold higher magnification are depicted in the insets. (c and d) Common carotid artery size (external elastic lamina or EEL perimeter; c) and wall (medial) thickness (d) was determined by image analysis software in WT, CXCR3$^{-/-}$, IL-1R$^{-/-}$, IL-6$^{-/-}$, TNFR1/R2$^{-/-}$, and iNOS$^{-/-}$ mice. Data are means ± SE (n = 9–10 pooled from six operative sessions). *, P < 0.05; **, P < 0.001, KO versus WT.

Flow-mediated vascular remodeling was believed to be an intrinsic property of the vessel wall. Recent work has challenged this paradigm with the observation that perivascular macrophages are necessary for enlargement or shrinkage of rodent carotid and mesenteric arteries as a result of increased or decreased blood flow, respectively (Bakker et al., 2008; Tang et al., 2008; Nuki et al., 2009). Rapid superoxide-initiated cytokine and chemokine production by vessel wall cells is followed by transient accumulation and activation of macrophages. Both phases are dependent on the expression of the adaptor molecule myeloid differentiation protein 88 (MyD88) and both are required for changes in vessel size (Tang et al., 2008). However, previous investigations have not identified specific inflammatory mediators with nonredundant roles in animal models of flow-mediated vascular remodeling.

Macrophages display great plasticity and are involved in host defense as well as homeostatic processes, such as wound healing and tissue remodeling (Mosser and Edwards, 2008). In keeping with multiple functions, macrophages and their monocyte precursors are heterogeneous (Gordon and Taylor, 2005). Further phenotypic polarization with distinct functional programs can be induced in macrophages by environmental stimuli that are generated after infection or tissue injury (Gordon and Taylor, 2005; Martinez, et al., 2008; Mosser and Edwards, 2008). Classical activation by prototypical stimuli of IFN-γ or LPS gives rise to M1 polarized macrophages with potent microbicidal and proinflammatory properties, including expression of inducible nitric oxide synthase (iNOS) and TNF production. In contrast, alternative activation by IL-4 or IL-13 gives rise to M2 polarized macrophages with enhanced capacity for tissue repair, for example, through secretion of MMPs and FXIIIA. A variety of other signals, such as immune complexes, IL-10, TGF-β, and glucocorticoids, generate variant polarized M3 macrophages with primary immunoregulatory roles as a result of IL-10 production.

Chemokine receptor expression contributes to the preferential trafficking of various monocyte subsets to tissues under physiological and pathological conditions. Longer-lived resident monocytes are CCR2^{-} and CX$_3$CR1^{high}, whereas short-lived inflammatory monocytes are CCR2^{+} and CX$_3$CR1^{low} (Geissmann et al., 2003). Among other homing receptors, monocytes are dependent on CCR2, CCR5, and CX$_3$CR1 to gain entry into atherosclerotic plaques of the artery wall (Tacke et al., 2007; Combadière et al., 2008; Saederup et al., 2008) and CX$_3$CR1 is also necessary for monocyte trafficking to the intima of aged nonatherosclerotic aortas (Liu et al., 2008). Homing requirements or retention signals for monocytes to the arterial adventitia have not been described. CXCR3, the receptor for IP-10 (IFN-γ–induced protein of 10 kD; also designated CXCL10) and monokine induced by IFN-γ (Mig; also designated CXCL9), is well characterized as a marker of activated and memory T cells. However, it has been known since the early descriptions of these molecules that CXCR3 is also expressed by monocytes/macrophages and that IP-10 will promote their recruitment (Luster and Leder, 1993; Taub et al., 1993; Luster et al., 1995). Finally, certain chemokines, such as CCR5 ligands, also contribute to macrophage activation (Zhou et al., 1998), although CXCR3 ligands have not previously been shown to play such a role. In this paper, we explain that the expression of CXCR3 by macrophages is necessary for flow-mediated inward vascular remodeling and that CXCR3 signaling contributes both to macrophage accumulation in the adventitia and to a limited but unique pattern of macrophage activation in response to altered hemodynamic stresses.

RESULTS

CXCR3 is necessary for flow-mediated inward vascular remodeling

To gain mechanistic insight into our previous observation that the expression of IP-10, Mig, IL-1β, IL-6, TNF, and iNOS is induced within conduit arteries in response to outflow reduction (Tang et al., 2008), we investigated if any of these proinflammatory factors are necessary for flow-mediated vascular remodeling. To test the role of IP-10 and Mig, we compared adaptive vascular remodeling in WT versus CXCR3-deficient ($CXCR3^{-/-}$) mice by measuring common carotid artery size and wall thickness at 2 wk after left external carotid artery ligation (Fig. 1 a). In WT mice, the left common carotid arteries displayed a 10–15% reduction in external perimeter, whereas medial thickness remained unchanged compared with the right common carotid arteries from the unligated side (Fig. 1, b–d). Strikingly, left common carotid arteries in $CXCR3^{-/-}$ mice did not inwardly remodel but responded by medial thickening instead. In contrast, mice with a deficiency of other proinflammatory factors induced by decreased blood flow (or with a deficiency of their receptors), such as IL-1R, IL-6, TNFR1/R2, and iNOS, showed similar vascular remodeling responses to that in WT mice, except for modestly less vessel shrinkage in $IL\text{-}6^{-/-}$ mice (Fig. 1 d). These results suggest a nonredundant role for CXCR3 ligands, such as IP-10 and Mig, in adaptive vascular remodeling that is not a general feature of other proinflammatory factors induced by perturbations in blood flow.

Adoptive transfer of WT myeloid cells to $CXCR3^{-/-}$ recipients restores flow-mediated inward vascular remodeling responses

Although CXCR3 is known to be expressed by both mouse T cells and macrophages (Luster and Leder, 1993; Taub et al., 1993; Luster et al., 1995), we have previously shown that vessel shrinkage in response to decreased blood flow is dependent on macrophages and not T cells (Tang et al., 2008). Therefore, we tested if monocytes from WT mice were sufficient to restore flow-mediated vascular remodeling in $CXCR3^{-/-}$ recipients. We were unable to achieve detectable adoptive transfer of blood monocytes, likely because of limited yield (Fig. S1). Larger numbers of bone marrow myeloid cells could be obtained after density centrifugation and immunomagnetic bead depletion of lymphoid cells and erythrocytes. The enriched cell population from WT mice was 95% positive for the myeloid cell marker CD11b and 60% positive for CXCR3, albeit at relatively low levels (Fig. 2 a). CXCR3 expression by the selected bone marrow cells was limited to Ly-$6C^+$ monocytes (Fleming et al., 1993) and was not detectable on small numbers of contaminating Ly-$6G^+$ granulocytes or $CD42d^+$ platelets (Fig. S2). Adoptively transferred bone marrow myeloid cells persisted in the circulation of WT and $CXCR3^{-/-}$ hosts for at least 3 d (Fig. S1), which was the peak period of perivascular macrophage recruitment in this model (Tang et al., 2008). We also used polymorphic determinants to the CD45 leukocyte common marker to confirm that donor cells

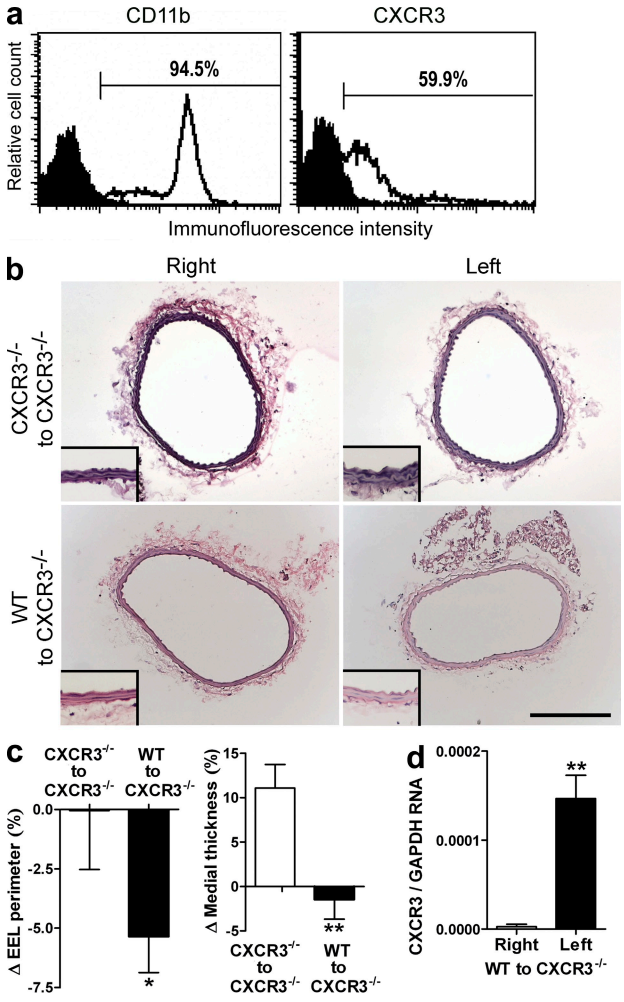

Figure 2. WT myeloid cells restore flow-mediated inward vascular remodeling in $CXCR3^{-/-}$ mice. (a) Bone marrow myeloid cells were negatively selected using density centrifugation and immunomagnetic beads and analyzed by FACS for CD11b and CXCR3 expression. (b) Representative photomicrographs of hematoxylin and eosin–stained transverse sections of the right (unligated side) and left (ligated side) common carotid arteries from $CXCR3^{-/-}$ animals that received 2.7×10^6 bone marrow monocytes i.v. from $CXCR3^{-/-}$ mice or from WT mice 12 h before ligation of the left external carotid artery. Bar, 200 µm. The vessel walls at twofold higher magnification are depicted in the insets. (c) Common carotid artery size (external elastic lamina or EEL perimeter) and wall (medial) thickness was determined by image analysis software in these animals. Data are means ± SE (n = 9–10 pooled from two operative sessions). *, $P < 0.05$; **, $P < 0.001$, WT to $CXCR3^{-/-}$ versus $CXCR3^{-/-}$ to $CXCR3^{-/-}$. (d) CXCR3 transcripts were quantified by real-time PCR and normalized to GAPDH from left and right common carotid arteries of $CXCR3^{-/-}$ mice at 3 d after adoptive transfer of WT bone marrow myeloid cells and left external carotid artery ligation. Data are means ± SE (n = 8 from one operative session). **, $P < 0.001$, left versus right.

tracked to the remodeling vessel wall in WT and $CXCR3^{-/-}$ hosts (Fig. S1). i.v. administration of bone marrow myeloid cells from $CXCR3^{-/-}$ donors to $CXCR3^{-/-}$ recipients did not alter the abnormal response of absent inward remodeling and aberrant medial thickening in common carotid arteries

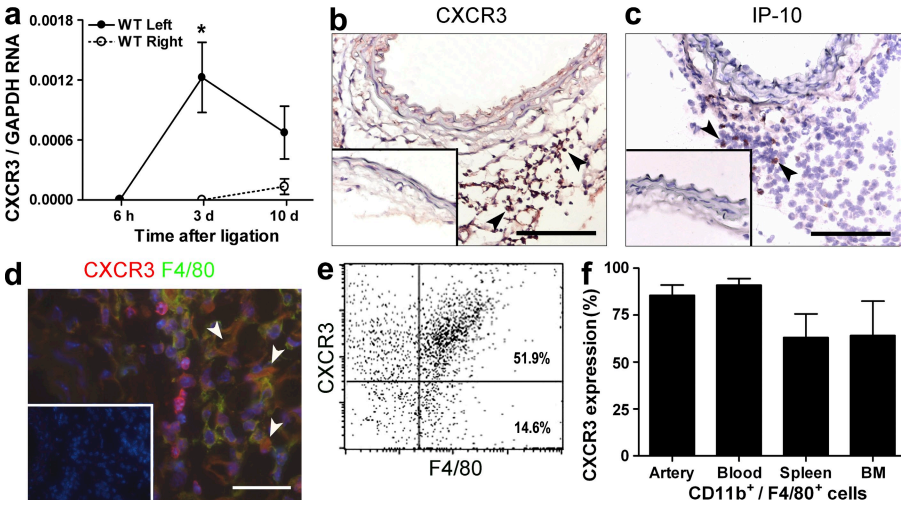

Figure 3. CXCR3 is expressed by artery-associated macrophages. (a) CXCR3 transcripts were quantified by real-time PCR and normalized to GAPDH from left and right common carotid arteries of WT mice at 6 h ($n = 10$), 3 d ($n = 9$), and 10 d ($n = 4$) after left external carotid artery ligation. Data are means ± SE (pooled from three operative sessions). *, $P < 0.05$, left versus right. (b and c) CXCR3 (b) and IP-10 (c) immunohistochemical reactivity (brown, arrowheads) in left common carotid arteries at 3 d after outflow reduction. Bars, 100 µm. Absent immunostaining in right common carotid arteries is shown in insets. (d) F4/80 (green) and CXCR3 (red) immunofluorescence signal in left common carotid artery at 3 d after outflow reduction. The overlapping dual signal (orange) is marked by arrowheads. Bar, 50 µm. Irrelevant isotype-matched antibody reactivity is depicted in the inset. (e) Cells were isolated from common carotid arteries at 3 d after partial outflow ligation using CD11b antibody-coated magnetic beads and analyzed by flow cytometry for CXCR3 and F4/80 expression. (f) CXCR3 expression by common carotid artery, blood, spleen, and bone marrow (BM) CD11b-selected F4/80-expressing cells. Data are means ± SE ($n = 4$ pooled from four independent experiments).

after external carotid artery ligation (Fig. 2, b and c), which was similar to that seen in CXCR3$^{-/-}$ mice without adoptive transfer of cells. In contrast, adoptive transfer of bone marrow myeloid cells from WT donors to CXCR3$^{-/-}$ recipients restored the phenotype of inward remodeling without medial thickening in response to outflow reduction, as in WT mice. CXCR3 was detected in the ligated, but not unligated, carotid arteries of CXCR3$^{-/-}$ recipients of WT myeloid cells (Fig. 2 d), confirming selective homing of the adoptively transferred cells to the remodeling vessel. These experiments implicate monocytes/macrophages as relevant cell types involved in CXCR3-dependent flow-mediated vascular remodeling.

CXCR3 is expressed in the adventitia of remodeling arteries

Because CXCR3 is necessary for vascular remodeling, we examined for its expression within the vessel wall of WT animals. Quantitative PCR analysis showed a time-dependent increase in CXCR3 transcripts within common carotid arteries after external carotid artery ligation, with peak expression at 3 d (Fig. 3 a). Immunohistochemical analysis verified the presence of CXCR3 and one of its ligands, IP-10, within the adventitia of remodeling arteries (Fig. 3, b and c). These results mirrored our previous finding that macrophages constitute the major population of artery-associated leukocytes in this model, with peak accumulation between 3 and 7 d after outflow reduction (Tang et al., 2008), and the expression of CXCR3 largely coincided with that of the macrophage marker F4/80 by immunofluorescence imaging (Fig. 3 d). However, not all F4/80$^+$ cells expressed CXCR3 and certain CXCR3$^+$ cells did not express F4/80. We quantified the expression of these markers by flow cytometric analysis of myeloid cells selected by CD11b antibody-coated magnetic beads from various sites (initial selection of relevant cells with immunomagnetic beads was necessary to avoid confounding signals from excessive debris in enzyme-digested artery preparations). The majority of adventitial macrophages, defined as CD11b-selected F4/80$^+$ cells, expressed CXCR3 as did circulating monocytes with the same surface markers (Fig. 3, e and f). The spleen and bone marrow contained fewer such cells, although these differences did not achieve statistical significance. Thus, CXCR3 expression is widely detected on diverse populations of F4/80$^+$ monocytes/macrophages.

Increased CXCR3 expression by Gr1^{low} perivascular macrophages

We further assessed the relative expression of CXCR3 by various populations of monocytes and macrophages defined by the Gr1 marker using flow cytometric analysis. Antibodies to the Gr1 determinant react with both Ly-6C (expressed by monocytes and granulocytes) and Ly-6G (expressed by granulocytes but not monocytes), and low versus high expression of Gr1 characterizes distinct subpopulations of mouse blood monocytes and plaque-infiltrating macrophages (Sunderkötter et al., 2004; Tacke et al., 2007). Two separate groups of CD11b-selected F4/80$^+$ blood monocytes were identified by low versus high Gr1 expression with modest surface expression of CXCR3 (Fig. 4 a, R1 and R2). In contrast, CD11b-selected F4/80$^-$ Gr1^{high} cells had little CXCR3 expression (Fig. 4 a, R3). Both the Gr1^{high} cell populations (R2 and R3) expressed Ly-6C, but not Ly-6G, identifying them as monocytes (Fig. S3). The F4/80$^-$ population (R3) likely represents monocytes recently emigrated from bone marrow or spleen. Artery-infiltrating macrophages had increased F4/80 expression, far fewer Gr1^{high} cells, more frequent Gr1^{low} cells, and 10-fold greater CXCR3 expression as compared with blood monocytes (Fig. 4 b). CD11b-selected F4/80$^-$ Gr1$^+$ cells were not detected within the vessel wall. Forward versus side scatter profiles revealed two populations of small and large artery-associated macrophages with overlapping expression patterns and less than twofold differences for F4/80, Gr1, and

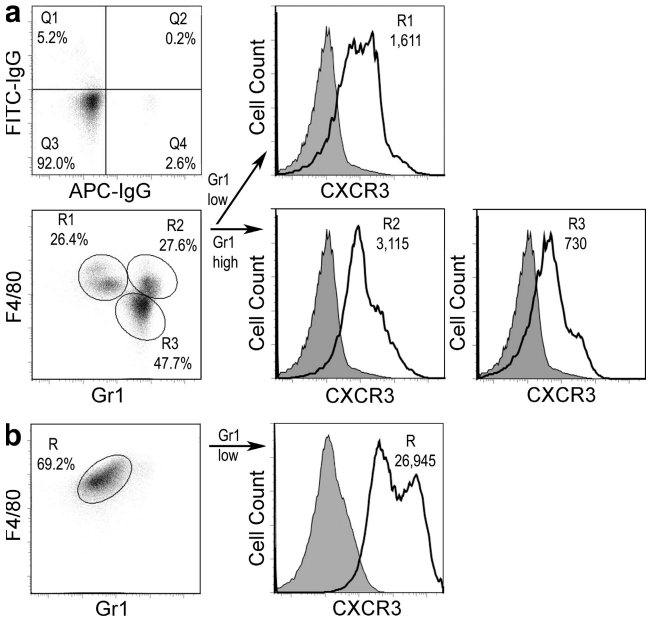

Figure 4. CXCR3 expression by Gr1-defined populations of blood monocytes and artery macrophages. Cells were isolated from blood (a) or left common carotid arteries (pooled from 22 mice; b) at 3 d after partial outflow ligation using CD11b antibody-coated magnetic beads and analyzed by flow cytometry for control IgG reactivity or F4/80 and Gr1 expression, which delineated three discrete populations of myeloid cells. Their frequency is shown, calculated as the percentage of total cells. The Gr1-defined cell populations were further analyzed for CXCR3 expression (open histograms) or irrelevant isotype-matched antibody reactivity (shaded histograms), and the mean fluorescence intensity is shown. Data are representative of three independent experiments.

CXCR3 (Fig. S4). The flow cytometry data indicate that a unique subtype of macrophage accumulates around the vessel wall in response to decreased blood flow, and a distinguishing feature of the remodeling-associated macrophage is the higher expression of CXCR3.

Perivascular accumulation of macrophages after decreased blood flow is CXCR3 dependent

Having shown that macrophages associated with remodeling arteries express CXCR3, we next investigated if CXCR3 signaling contributes to monocyte trafficking to the vessel wall. The early induction of IP-10 and Mig transcripts in vascular cells at 6 h after external carotid artery ligation did not differ between WT and CXCR3$^{-/-}$ mice (Fig. 5 a). However, the accumulation of F4/80 transcripts was less in common carotid arteries from CXCR3$^{-/-}$ mice compared with WT mice at 3 d (Fig. 5 b) and 7 d (not depicted). We verified decreased recruitment and/or retention of macrophages in CXCR3$^{-/-}$ animals by counting F4/80^{+} cells in artery sections (Fig. 5, c and d). To determine if CXCR3 signaling was sufficient for monocyte infiltration of the vessel wall independent of lymphocyte trafficking, we applied IP-10 to the tissues surrounding the common carotid artery of RAG1$^{-/-}$ mice deficient in T and B cells. This resulted in infiltration of F4/80^{+} cells to

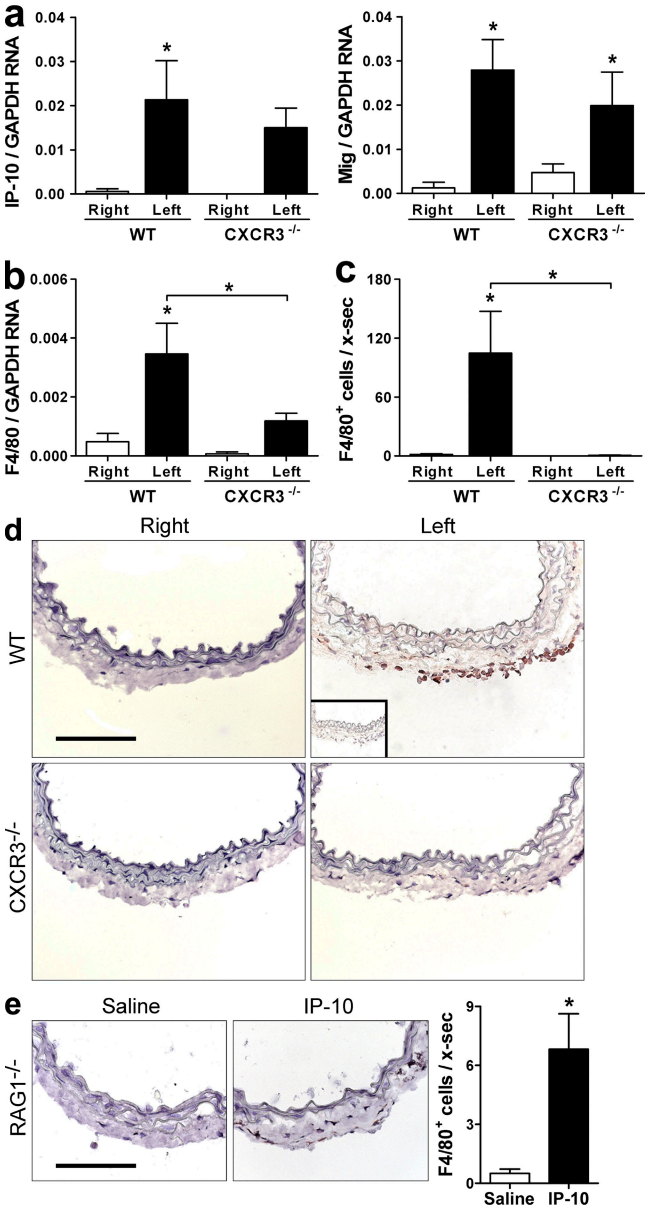

Figure 5. CXCR3 is necessary and sufficient for perivascular macrophage accumulation. (a and b) Transcripts for IP-10 and Mig at 6 h (a) and F4/80 at 3 d (b) were quantified by real-time PCR and normalized to GAPDH from right and left common carotid arteries of WT and CXCR3$^{-/-}$ mice after left external carotid artery ligation (n = 8–10 pooled from four operative sessions). (c) The number of F4/80^{+} cells per vessel cross section (x-sec) were counted from immunohistochemical analyses of common carotid arteries at 3 d after outflow reduction (n = 8 pooled from two operative sessions). (d) Representative photomicrographs from c are shown. Bar, 100 µm. Irrelevant isotype-matched antibody reactivity is depicted in the inset. (e) F4/80^{+} cells per vessel cross section were also counted from common carotid arteries infiltrated with saline or IP-10 at 300 ng/µl for 3 d in RAG1$^{-/-}$ mice (n = 6 pooled from two operative sessions). Bar, 100 µm. Data are means ± SE. *, P < 0.05, left versus right, CXCR3$^{-/-}$ versus WT, or IP-10 versus saline.

the adventitia of IP-10–treated, but not contralateral, vehicle-treated vessels at 3 d (Fig. 5 e). Macrophages were not detected within the media or intima of the arteries similar to the

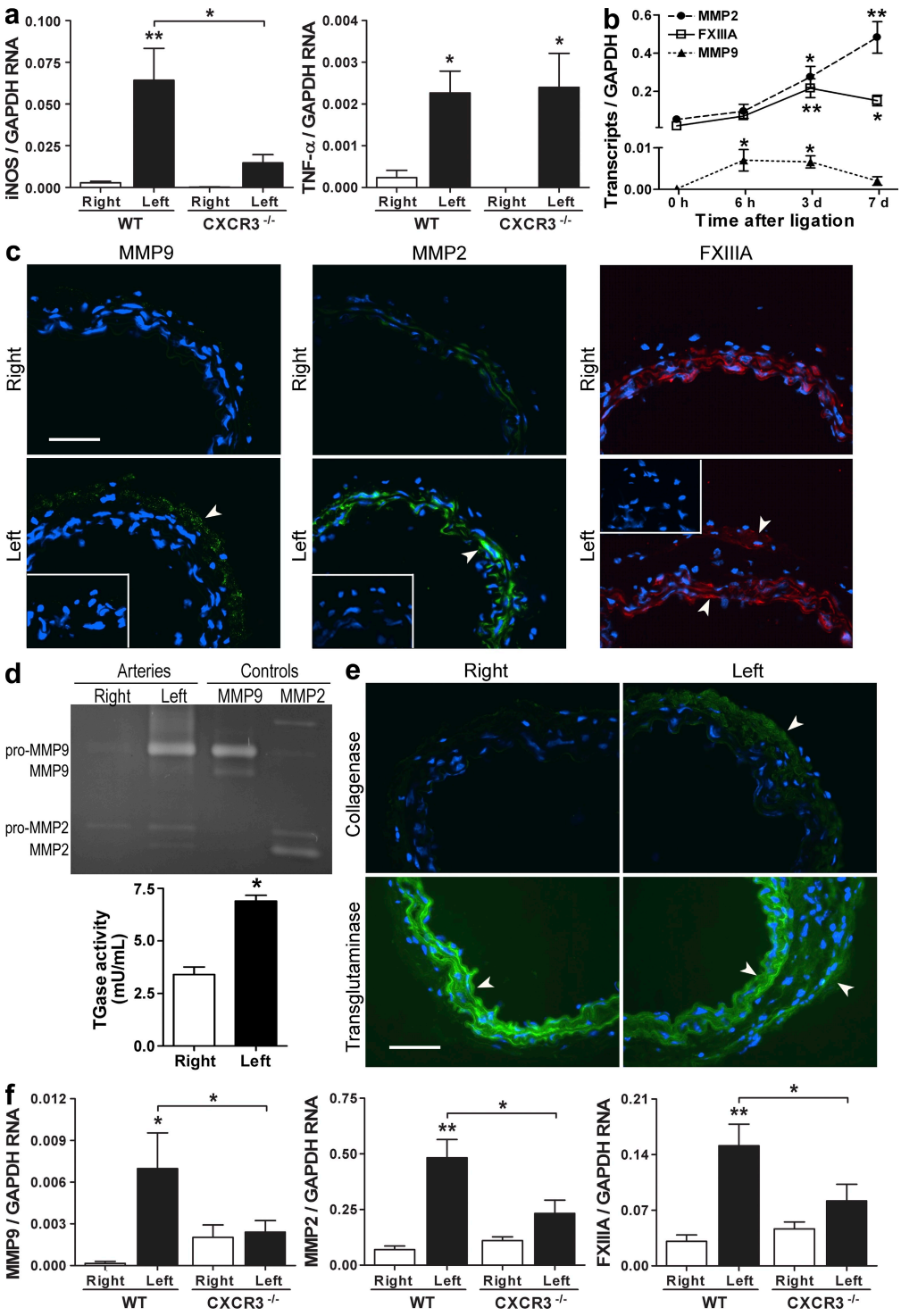

Figure 6. Production of macrophage mediators of vascular inflammation and remodeling after decreased flow is CXCR3 dependent. (a) Transcripts for iNOS and TNF were quantified by real-time PCR and normalized to GAPDH from right and left common carotid arteries of WT and CXCR3$^{-/-}$ mice at 3 d after left external carotid artery ligation (n = 9 pooled from two operative sessions). (b) Transcripts for MMP9, MMP2, and FXIIIA in left common carotid arteries of WT mice at 0 h, 6 h, 3 d, and 7 d after operation (n = 9–10 pooled from four operative sessions). (c) Immunofluorescence analyses of MMP9, MMP2, and FXIIIA expression in common carotid arteries at 3 d after outflow reduction, orientation with lumen below and adventitia above. Arrowheads mark immunofluorescence signal. Bar, 50 µm. Irrelevant isotype-matched antibody reactivity is depicted in the insets. (d) Collagenase and transglutaminase (TGase) activity in lysates of common carotid arteries at 3 d after outflow reduction. Standards of purified MMP9 and MMP2 indicate pro- and active MMP bands in gel zymogram. n = 3 from one operative session in transglutaminase assay. (e) In situ collagenase and transglutaminase activity in common carotid arteries at 3 d after outflow reduction. Enzyme activity is colored green and is marked by arrowheads. Bar, 50 µm. (f) Transcripts

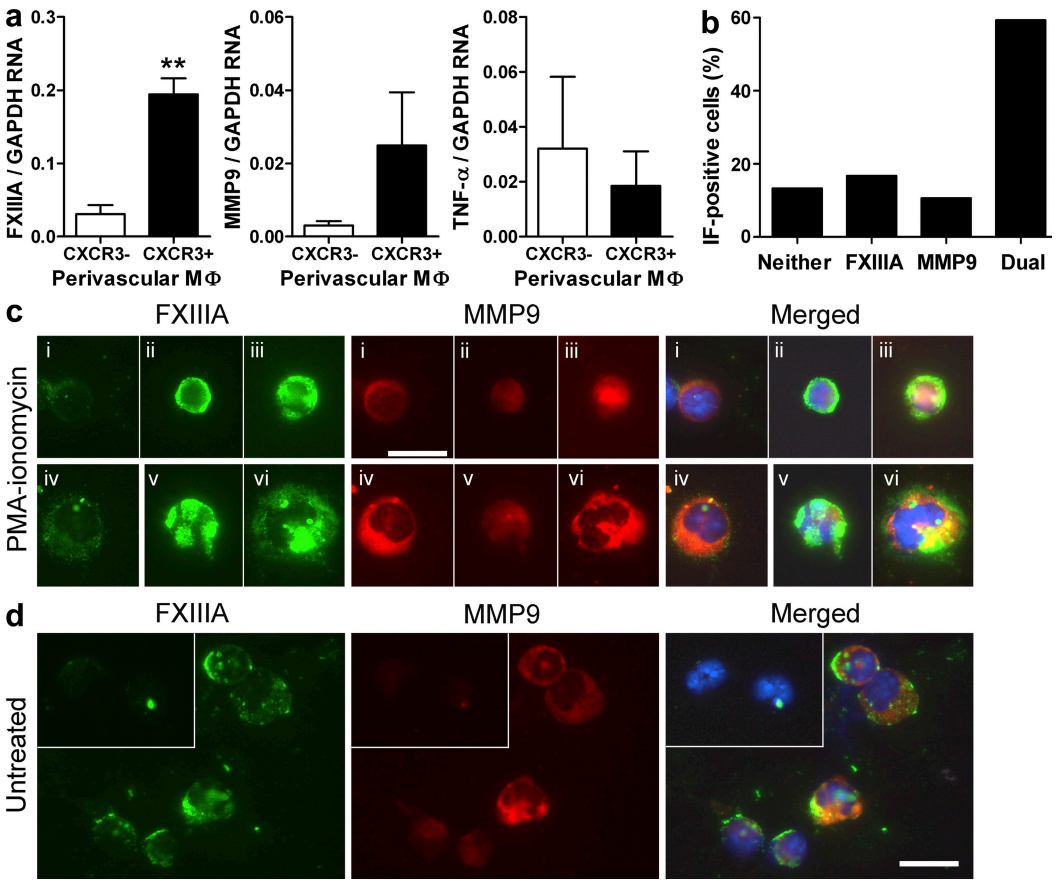

Figure 7. FXIIIA production is limited to CXCR3-expressing macrophages and FXIIIA is frequently coexpressed with MMP9 in situ. (a) Perivascular macrophages were isolated with anti-CD11b–coated magnetic beads from common carotid arteries 3 d after ipsilateral external carotid artery ligation. CXCR3$^-$ and CXCR3$^+$ F4/80-expressing macrophages were sorted by flow cytometry, RNA was extracted from an equal number of cells, and FXIIIA, MMP9, and TNF transcripts were measured by real-time PCR (n = 5–7 pooled from three independent experiments). Data are means ± SE. **, $P < 0.001$, CXCR3$^+$ versus CXCR3$^-$. (b) Alternatively, CD11b-selected CD3$^-$/B220$^-$/CD11c$^-$ adventitial macrophages were isolated by immunomagnetic beads and flow cytometry from 18 remodeling arteries (generated in one operative session) at 3 d after operation, treated with PMA and ionomycin for 5 h, cytospins were prepared, and the expression of FXIIIA and MMP9 was analyzed by immunofluorescence (IF) microscopy and image analysis software from 134 images. (c) Representative photomicrographs are shown of predominantly MMP9-expressing (i and iv), predominantly FXIIIA-expressing (ii and v), and dual FXIIIA-MMP9-expressing (iii and vi) small (top) and large (bottom) macrophages. (d) Similar analysis was performed on cytospins of untreated adventitial macrophages. Bar, 15 µm. Irrelevant isotype-matched antibody reactivity is depicted in the insets. Data are representative of two independent experiments.

limited distribution noted after blood flow reduction. These results demonstrate that CXCR3 was necessary and sufficient for perivascular macrophage accumulation.

Production of macrophage mediators of vascular remodeling after decreased blood flow is CXCR3 dependent

We further investigated if CXCR3 signaling was required for the production of macrophage mediators of vascular inflammation and remodeling. iNOS, but not TNF, transcripts were diminished in common carotid arteries from CXCR3$^{-/-}$ mice compared with WT mice at 3 d after outflow reduction (Fig. 6 a), which was previously documented as the time of peak expression for these inflammatory mediators in this experimental model (Tang et al., 2008). Because our results showed that neither iNOS nor TNF played nonredundant roles in inward vascular remodeling (Fig. 1 d), we also assessed the expression of other effector molecules that have been associated with extracellular matrix turnover and flow-mediated vascular remodeling, such as the proteinases, MMP2 and MMP9, and the transglutaminase FXIIIA (Bassiouny et al., 1998; Galis et al., 2002; Bakker et al., 2006). In common carotid arteries of WT mice, MMP9 transcripts that were undetectable preoperatively were induced early between 6 h and 3 d after external carotid artery ligation, whereas the basal expression of MMP2 and FXIIIA transcripts was upregulated later between 3 and 7 d after operation (Fig. 6 b).

for MMP9 at 6 h, MMP2 at 7 d, and FXIIIA at 7 d after operation in common carotid arteries of WT and CXCR3$^{-/-}$ mice (n = 7–10 pooled from two operative sessions). Data are means ± SE. *, $P < 0.05$; **, $P < 0.01$, left versus right, CXCR3$^{-/-}$ versus WT, or after ligation versus 0 h.

By immunofluorescence imaging, the induction of MMP9 expression was only detected in the adventitia, whereas the up-regulation of MMP2 expression was restricted to the media at 3 d after outflow reduction (Fig. 6 c). In contrast, FXIIIA expression was expressed in both the media at baseline and was also associated with perivascular infiltrating cells (Fig. 6 c). We confirmed increased gelatinase activity as a result of MMP9 and MMP2 expression in remodeling arteries by gel and in situ zymography and increased transglutaminase activity within the adventitia, in addition to basal medial activity, after decreased blood flow (Fig. 6, d and e). The early accumulation of MMP9 transcripts and the later accumulation of MMP2 and FXIIIA transcripts were diminished in common carotid arteries from the ligated side of CXCR3$^{-/-}$ mice compared with WT mice (Fig. 6 f). These results do not exclude the possibility that the diminished expression of factors produced by activated macrophages was entirely the result of decreased monocyte recruitment and/or macrophage retention.

FXIIIA is selectively produced by CXCR3^{+} perivascular macrophages and is frequently coexpressed with MMP9 in situ

To determine if CXCR3 signaling may contribute to macrophage activation independent of chemoattractant effects, we first assessed the products of different macrophage populations defined by CXCR3 expression from remodeling common carotid arteries of WT mice. The abundance of FXIIIA transcripts was significantly higher in CXCR3-expressing CD11b-selected F4/80^{+} cells, and a similar trend for MMP9 transcripts did not achieve statistical significance (Fig. 7 a). In contrast, TNF was detected in both CXCR3^{+} and CXCR3^{-} macrophages and MMP2 transcripts were not detected in either macrophage population. To examine the production of FXIIIA and MMP9 at the single cell level, we analyzed CD11b-selected CD3^{-}/B220^{-}/CD11c^{-} perivascular macrophages by immunofluorescence microscopy. There was a heterogeneous expression pattern in macrophages activated with PMA/ionomycin ex vivo with minor populations expressing predominantly FXIIIA, predominantly MMP9, or neither molecule, although the majority of cells displayed dual FXIIIA and MMP9 immunoreactivity (Fig. 7 b). These diverse macrophage subgroups contained both smaller cells with more rounded nuclei and larger cells with kidney- and horseshoe-shaped nuclei (Fig. 7 c). Similar findings with lesser intensity of signal were seen in untreated adventitial macrophages (Fig. 7 d). These data suggested that many CXCR3-expressing remodeling-associated macrophages displayed both proteinase and transglutaminase activities.

CXCR3 signaling induces FXIIIA production by isolated macrophages in vitro

We next examined for direct evidence of IP-10 effects on macrophages in vitro. Bone marrow monocytes were differentiated in culture to a macrophage-type phenotype in the presence of macrophage (M) CSF–conditioned medium for 7–10 d, which increased CXCR3 expression (unpublished data), before treatment with various proinflammatory agents. IP-10 selectively induced the expression of FXIIIA transcripts, whereas a prototypical alternative activator of macrophages, IL-4, and a prototypical classical activator of macrophages, LPS, induced the expression of MMP9 and TNF transcripts, respectively (Fig. 8 a). We verified the IP-10–mediated up-regulation of FXIIIA transcripts with additional dose-response experiments, as well as induction of FXIIIA protein by Western blotting which was associated with increased transglutaminase activity (Fig. 8 b). Similarly, FXIIIA was induced by IP-10 in blood monocytes independent of the need for M-CSF–mediated differentiation (Fig. S5). In contrast, IL-4 and LPS diminished the basal expression of FXIIIA by bone marrow–differentiated macrophages and inhibited the effects of IP-10 but not vice versa (Fig. 8 c). Further analyses were performed for other markers of alternative and classical macrophage activation. As expected, IL-4 up-regulated arginase I, Ym1, and Fizz1 transcripts (Nair et al., 2003), whereas LPS induced iNOS transcripts. IP-10 at 300 ng/ml for 72 h did not significantly affect the expression of any of these molecules (Table S1). Unlike IL-4 or LPS, IP-10 did not modulate the production of the immunoregulatory cytokine IL-10. Additionally, the expression of TGM2, an alternative source of transglutaminase activity in remodeling vessels, was not modulated by IP-10 but was inhibited by IL-4 and LPS. We verified that the IP-10–mediated induction of FXIIIA was CXCR3 dependent, which is in contrast to the qualitatively similar effects of IL-4 and LPS on WT cells in the presence of CXCR3 blocking antibodies or on CXCR3$^{-/-}$ cells (Fig. 8 d). Together, these in vitro data demonstrate that CXCR3 signaling contributes to selective and unique features of macrophage activation in the absence of other cell types.

Human perivascular macrophages express CXCR3

To determine if our findings in mouse models may be of relevance in human biology, we examined the phenotype of perivascular macrophages in clinical specimens. CD11b^{+} cells were selected by magnetic beads from blood and aortic adventitia and analyzed by flow cytometry. CXCR3 was expressed by a distinct population of CD11b-selected CD14^{+} adventitial macrophages but not by circulating monocytes (Fig. 9 a). CD11b^{+}/CD14^{+}/CXCR3^{+} perivascular cells did not express lymphocyte or neutrophil markers and were CD3^{-}/CD15^{-}/CD19^{-}/CD56^{-}/CD177^{-} (Fig. S6). The frequency of CD11b^{+}/CD14^{+}/CXCR3^{+} cells was higher in the adventitia of aneurysmal aortas than of nonaneurysmal aortas (Fig. 9 a). Further analysis of CD11b-selected adventitial cells revealed that CXCR3 was more frequently expressed by macrophages characterized by a CD14^{+}/CD16^{+} resident phenotype than by a CD14^{+}/CD16^{-} inflammatory phenotype (Fig. 9 b). The expression of the scavenger receptor CD163 was also greater in CD14^{+}/CD16^{+} than in CD14^{+}/CD16^{-} perivascular macrophages (Fig. 9 b). Finally, there were more numerous CD68^{+} macrophages resident in adventitia at sites of disturbed blood flow, such as the common carotid

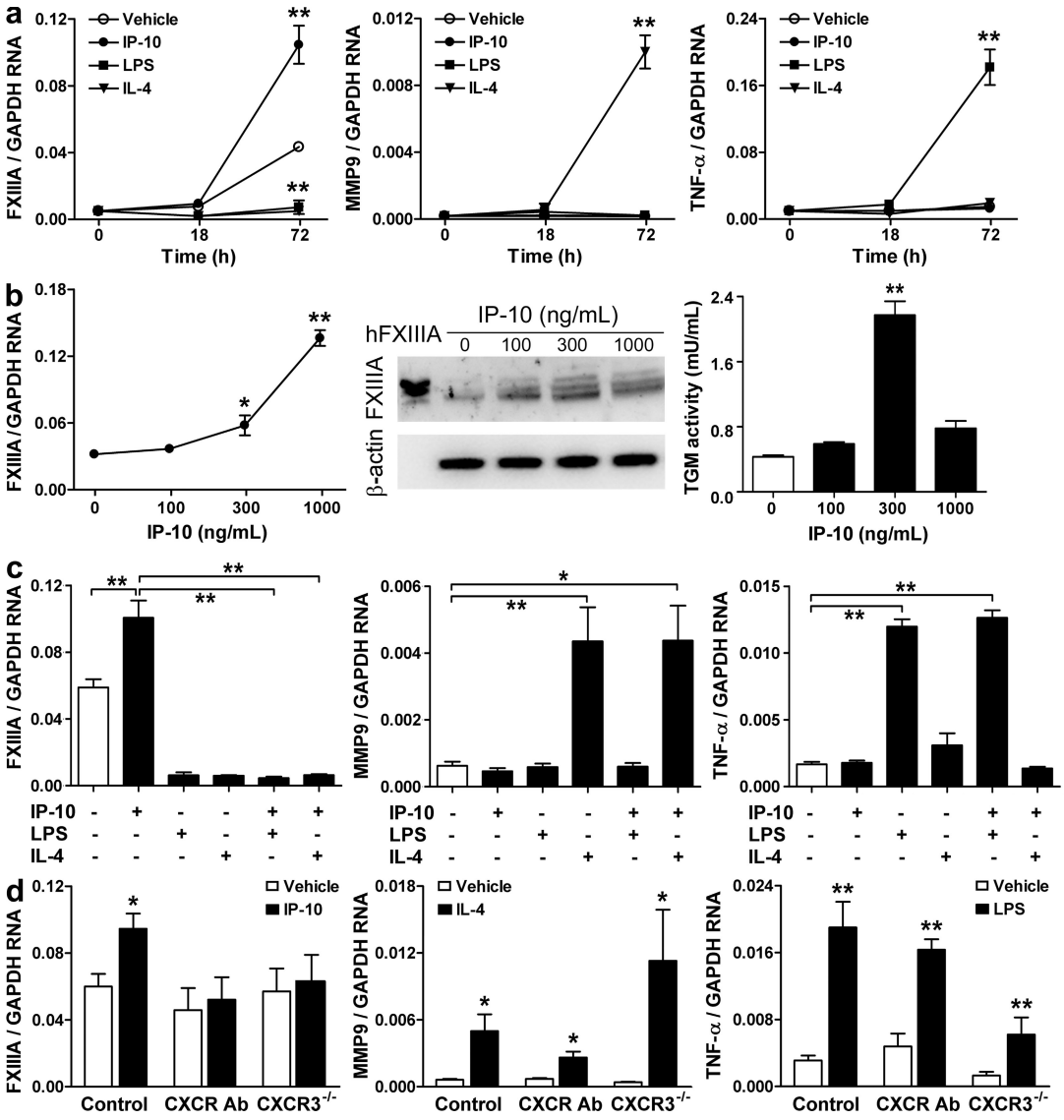

Figure 8. IP-10 induces FXIIIA expression in cultured macrophages. (a) Bone marrow monocytes were matured in culture in the presence of M-CSF–enriched medium for 7–10 d before treatment with IP-10 at 300 ng/ml, LPS at 10 ng/ml, or IL-4 at 10 ng/ml for various times, and FXIIIA, MMP9, and TNF transcripts were measured ($n = 4$ pooled from four independent experiments). (b) The cells were also treated with IP-10 at various concentrations. FXIIIA transcripts were measured by quantitative PCR ($n = 3$ pooled from three independent experiments) at 72 h. FXIIIA protein was assessed by immunoblotting of cell lysates at 96 h, purified human FXIIIA (75 kD) was included at 100 ng/ml, β-actin expression was used as loading controls, and blots are representative of three independent experiments. Transglutaminase activity was determined in macrophage lysates after IP-10 treatment for 96 h ($n = 2$ pooled from two independent experiments). (c) Quantitative PCR was also performed after treatment with single or combined proinflammatory factors at 72 h ($n = 6–8$ pooled from three independent experiments). (d) FXIIIA, MMP9, and TNF transcripts were measured in macrophages from WT mice after treatment with IP-10, IL-4, or LPS in the presence of CXCR3 blocking antibody (Ab) at 10 µg/ml versus irrelevant isotype-matched IgG or in macrophages from $CXCR3^{-/-}$ mice and compared with that of WT mice ($n = 6–12$ pooled from three independent experiments). Data are means ± SE. *, $P < 0.05$; **, $P < 0.001$, treated versus untreated, or single versus combined treatment.

artery bifurcation (carotid sinus), than at sites of laminar flow, for example, the midpoint of the common carotid artery (26.5 ± 3.2 vs. 14.5 ± 2.0 mm^{-3}, respectively; $P < 0.05$) with a higher expression of CXCR3 (Fig. 9 c). These data confirm that CXCR3 is expressed by a subset of human perivascular macrophages and that accumulation of this cell population spatially correlates with sites of disturbed hemodynamic stresses on the vessel wall.

DISCUSSION

In this study, we report several novel roles for CXCR3 in mouse systems: CXCR3 is necessary for flow-mediated inward vascular remodeling; CXCR3 is expressed by a subset of circulating monocytes and perivascular macrophages with resident phenotypic markers; CXCR3 is required for perivascular macrophage accumulation and activation after decreased blood flow; and CXCR3 signaling selectively induces FXIIIA

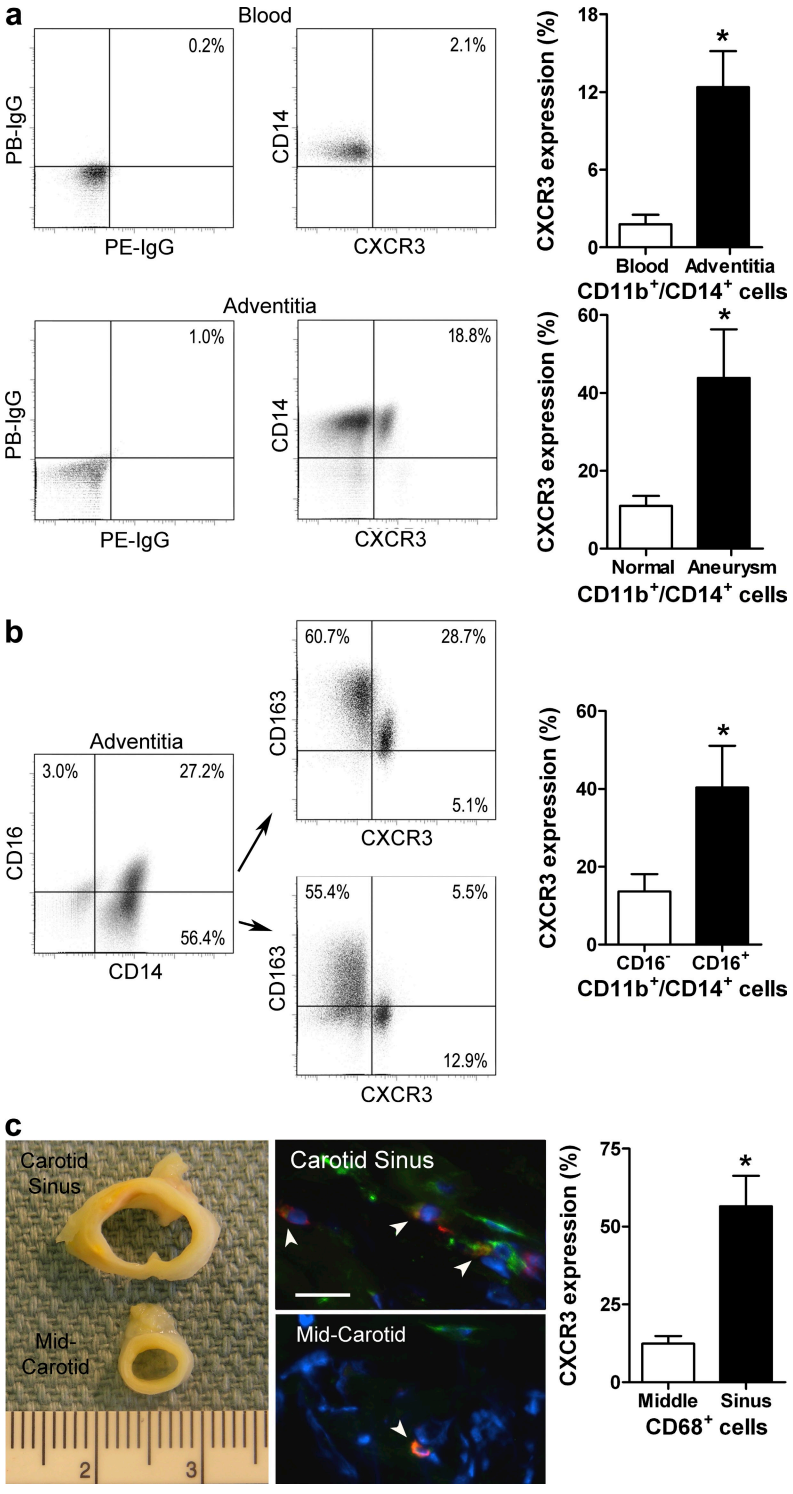

Figure 9. Human perivascular macrophages express CXCR3. (a) CD11b+ cells were isolated from blood or aortic adventitia using magnetic beads, analyzed by flow cytometry for control IgG reactivity or CD14 and CXCR3 expression, and a representative dot plot and combined results ($n = 4$) are shown. CXCR3 expression by perivascular macrophages was also compared between the nonaneurysmal ($n = 5$) and aneurysmal aortas ($n = 3$). (b) CD11b+/CD14+ adventitial cells were further analyzed for the CD16 resident macrophage marker in addition to CXCR3 and CD163 expression, and a representative dot plot and combined results ($n = 7$) are shown. (c) Distal (sinus) and mid-common carotid arteries ($n = 3$) were analyzed for CD68 (green) and CXCR3 (red) expression by immunofluorescence, and the frequency of CXCR3+/CD68+ cells (double-positive cells marked by arrowheads) were expressed as the percentage of total CD68+ cells. Bar, 25 µm. Data are means ± SE (each replicate is derived from a different donor and each specimen was processed independently). *, $P < 0.05$.

expression by monocytes and macrophages. We also find that CXCR3-expressing human macrophages of resident phenotype accumulate at sites of disturbed blood flow. These findings provide new insights into the mechanisms of macrophage-mediated vascular remodeling in response to hemodynamic forces and suggest that a unique macrophage phenotype is involved in homeostatic responses triggered by tissue stress.

In our previous study, we found two distinct roles for MyD88 in flow-mediated inward vascular remodeling (Tang et al., 2008). It was required both for ROS-initiated vascular cell inflammatory responses and consequent macrophage accumulation and for activation of macrophage effectors of vascular remodeling. We did not define inflammatory or remodeling mediators with nonredundant roles in this initial work. In our present study, we find that CXCR3 is necessary for perivascular macrophage recruitment in response to blood flow reduction and that IP-10 induces FXIIIA expression. The two studies are related in both phases of inward vascular remodeling. First, MyD88-dependent vascular cell inflammatory responses are required for the production of CXCR3 ligands. Second, both MyD88-dependent and CXCR3 signaling are required for production of macrophage mediators of vascular remodeling. The MyD88-dependent effectors of vascular remodeling are as yet undefined. FXIIIA is identified as a CXCR3-dependent macrophage product that is not induced by ligands that signal through MyD88, although it has not been proven to play an essential role in our model.

Although we have previously described the production of IP-10 and Mig during flow-mediated inward vascular remodeling, it was surprising to find a nonredundant role for their receptor CXCR3, as we had also found that this process is largely independent of T cells and only minimally reduced in RAG1$^{-/-}$ mice (Tang et al., 2008). CXCR3 is known to play an essential role in intimal remodeling in hypercholesterolemic mice (van Wanrooij et al., 2005, 2008; Veillard et al., 2005) and after wire-mediated injury of the mouse femoral artery (Schwarz et al., 2009).

However, the function of CXCR3 in these models of neointima formation is as a chemoattractant for T cells. Specifically, monocyte recruitment to atherosclerotic plaques is not reduced in hypercholesterolemic animals with genetic deficiency or pharmacologic inhibition of CXCR3 (van Wanrooij et al., 2005, 2008; Veillard et al., 2005). This discrepancy with our findings may reflect different homing requirements or retention signals for adventitial versus intimal compartments under physiological and pathological settings, respectively. Leukocyte–endothelial interactions are dependent on hemodynamic factors and the endothelial phenotype, which differ between adventitial microvessels and the lumen of conduit arteries (Langheinrich et al., 2007). Temporal and spatial variables may also play a role. Notably, the perivascular inflammation in response to altered shear stress in our model is transient and resolves without neointima formation after the adaptive changes in vessel size have occurred within 1–2 wk (Tang et al., 2008). The interpretation of our adoptive transfer experiments in which WT monocytes rescued the inward vascular remodeling phenotype in $CXCR3^{-/-}$ mice is limited by the caveats that negatively selected bone marrow myeloid cells may contain rare nonmonocyte precursor cells with sufficient proliferation potential to influence the results, small numbers of contaminating granulocytes that do not express CXCR3 may have nonredundant effects, and the initial perivascular accumulation of relatively few WT macrophages may secondarily recruit $CXCR3^{-/-}$ cells thus playing a critical but not sufficient role.

We document variable expression of CXCR3 by mouse $CD11b^+$ $F4/80^+$ cells from different anatomical sites. Robust expression of CXCR3 was previously reported for mouse thioglycollate-elicited peritoneal macrophages (Janatpour et al., 2001). In contrast, CXCR3 was undetectable in many analyses of human monocytes and macrophages (Janatpour et al., 2001; Katschke et al., 2001; Geissmann et al., 2003; Cho et al., 2007). We confirm that human circulating monocytes do not express CXCR3, but we demonstrate that perivascular macrophages, particularly of cells characterized by a $CD14^+/CD16^+$ resident phenotype (Geissmann et al., 2003), selectively express CXCR3 in addition to the scavenger receptor CD163 (Kim et al., 2006). Tissue macrophages that coexpress CD163 and FXIIIA have been described in human skin (Zaba et al., 2007). Because unstimulated human monocytes, unlike mouse myeloid cells, do not express detectable CXCR3, signaling by this receptor may recruit rare circulating precursors or contribute to the retention and activation of differentiated human tissue macrophages at sites of disturbed hemodynamic stresses. IP-10 elicits mouse monocyte recruitment in vivo (Luster and Leder, 1993; Taub et al., 1993, 1996), and deficient CXCR3 signaling is associated with diminished accumulation of macrophages in various mouse models of inflammation (Hancock et al., 2000; Janatpour et al., 2001; Waeckel et al., 2005; Heller et al., 2006; van Wanrooij et al., 2008). However, the interpretation of these findings is limited without confirmation of CXCR3 expression by the recruited macrophages and by not excluding indirect effects on monocyte trafficking by CXCR3-expressing T cells. More direct evidence of CXCR3-mediated effects includes chemotaxis of purified populations of human monocytes in response to IP-10 in vitro (Taub et al., 1993, 1996; Kohrgruber et al., 2004). We extend these observations by demonstrating a physiological role for CXCR3-mediated macrophage accumulation in adaptive vascular remodeling and show that IP-10 recruits monocytes to the arterial adventitia independent of lymphocytes in $RAG1^{-/-}$ mice.

Circulating monocytes and tissue macrophages, including those present in blood vessels, are characterized as long-lived resident cells or short-lived inflammatory cells with distinct migratory patterns (Geissmann et al., 2003). Resident macrophages have been described in the aortic adventitia of normocholesterolemic mice (Galkina et al., 2006), and macrophage-derived foam cells in developing atherosclerotic lesions do not derive from resident adventitial macrophages (Lessner et al., 2002). However, $Gr1^{low}$ resident monocytes that patrol the resting vasculature can rapidly invade the vessel wall in response to inflammatory signals (Auffray et al., 2007). We have not determined the origin of macrophages accumulating in remodeling arteries, a subject of future studies, although a 65-fold increase in cell number within 3 d of altered hemodynamic stresses (Tang et al., 2008) makes it unlikely that they are all derived from preexisting resident macrophages and suggests that the influx of cells mostly accrue from the circulation. Inflammatory macrophages, including those within atherosclerotic arteries, are described as $Gr1^{high}$ (Geissmann et al., 2003; Tacke et al., 2007), although it is known that the expression of Ly-6C decreases as monocytes remain in the circulation (Sunderkötter et al., 2004) and that adoptively transferred monocytes down-regulate Ly-6C expression after entering atherosclerotic aortic plaques (Swirski et al., 2007). Thus, $Gr1^{low}$ macrophages in the adventitia of remodeling arteries may be derived from circulating $Gr1^{high}$ cells that subsequently decreased the expression of this marker or, alternatively, may be selectively derived from circulating $Gr1^{low}$ cells. Our findings of smaller and larger perivascular macrophages are similar to previous descriptions of blood and spleen monocytes in which size and nuclei shape defined different cell differentiation states (Swirski et al., 2009).

In addition to its chemotactic effects, CXCR3 signaling is also known to play a role in the proliferation, effector cytokine production, and reactive oxygen species generation of T cells (Whiting et al., 2004; Schwarz et al., 2009). However, CXCR3 has not been described to contribute to macrophage activation. The differences in expression of macrophage mediators of inflammation and remodeling between WT and $CXCR3^{-/-}$ mice in our study may be entirely the result of differences in cell numbers, although the differential gene expression between $CXCR3^+$ and $CXCR3^-$ perivascular macrophages in WT mice and the effects of IP-10 on isolated monocytes and macrophages argue against this interpretation. We show induction of FXIIIA expression by IP-10 treatment in addition to the up-regulation of this molecule by M-CSF–dependent differentiation of mouse bone marrow–derived macrophages. LPS and IL-4 inhibit these responses, and the

cross-regulation of effector molecules by different macrophage activators is well established (Mosser and Edwards, 2008). IP-10 is strongly induced in macrophages by IFN-γ so that FXIIIA induction could arise from autocrine or paracrine signaling in M1 type activation. Alternatively, the characteristics of CXCR3-mediated macrophage activation may be considered to be partial M2 polarization even though there are striking differences with the phenotype induced by the prototypical alternative activator IL-4 in mouse macrophages, as it recapitulates IL-4–mediated induction of FXIIIA in human macrophages (Gratchev et al., 2005; Töröcsik et al., 2005; Martinez et al., 2008). The limited but unique pattern of macrophage activation by CXCR3 ligands, which is not seen with IL-4 or LPS, suggests a role for a macrophage population in the arterial wall that is neither M1 nor M2 and is responsible for adaptive vascular remodeling. M1- and M2-independent effects of another chemokine, PF4/CXCL4 (which shares binding sites with IP-10), have recently been described as M4 activation of blood-derived macrophages (Gleissner et al., 2010). Although the IP-10–dependent induction of FXIIIA in cultured macrophages was only severalfold, it was similar in magnitude to that in remodeling arteries. In a previous microarray study of human blood-derived macrophages, modest differences in gene expression were found in response to relatively high doses of MCP-1/CCL2 and GRO-α/CXCL1 without obvious polarization signatures (Cho et al., 2007). In vitro studies require comparatively high concentrations of IP-10 or other chemokines as a result of lower affinities for their cognate receptors than those of many proinflammatory cytokines. High local concentrations of IP-10 may be reached in vivo by binding to low-affinity nonspecific binding sites on surface proteoglycans, such as on endothelial cells (Ranjbaran et al., 2006). The activation of monocytes and macrophages by chemokines may also be dependent on their state of differentiation, and M-CSF has a significant transcriptional program (Martinez et al., 2006, Cho et al., 2007). The ability of CXCR3 ligands to both recruit and activate macrophages (this study) and to both recruit and activate lymphocytes (Whiting et al., 2004; Schwarz et al., 2009) qualifies these inflammatory mediators as alarmins or immune amplifiers (Oppenheim and Yang, 2005).

The production of diverse macrophage-derived factors are found in remodeling arteries, including products of M1 polarized macrophages, such as iNOS and TNF, and products of M2 polarized macrophages, such as MMP9 and FXIIIA (Galis et al., 2002; Bakker et al., 2006, 2008; Tang et al., 2008; Nuki et al., 2009). Indeed, TNF, IL-4, and TGF-β are all expressed in remodeling arteries after reduction of blood flow (Bakker et al., 2008) and may trigger classical activation, alternative activation, and deactivation of macrophages, respectively. Smooth muscle cell death, in addition to extracellular matrix degradation and cross-linking, occurs in inward vascular remodeling (Rudic et al., 2000; Tang et al., 2008) and, thus, the activity of both cytotoxic (M1) and tissue repair (M2) macrophages may be expected to play a role. The lack of nonredundant roles for TNF and iNOS in flow-mediated inward vascular remodeling is surprising given their essential functions in arterial remodeling in models of hypertension and graft arteriosclerosis, respectively, although these inflammatory mediators were described as T cell products in these studies (Koh et al., 2004; Guzik et al., 2007). Given its role in vascular smooth muscle cell proliferation (Selzman et al., 1999), one may speculate that the persistence of TNF production in CXCR3$^{-/-}$ animals in this study and in MyD88$^{-/-}$ animals or in monocyte-depleted animals in our previous study (Tang et al., 2008) may be responsible for the paradoxical medial thickening observed in the absence of inward vascular remodeling. We have not investigated if the artery-associated macrophages in our in vivo model are polarized into mutually exclusive subsets or whether single cells retain plasticity to secrete both M1 and M2 products. Recent work on heterogeneous macrophage subsets involved in tissue healing and remodeling after myocardial infarction showed both MMP activity and TNF production by all Ly-6C^{high} macrophages using single event histograms, suggesting dual production of M1 and M2 products in vivo (Nahrendorf et al., 2007). The paradigm of macrophage polarization requires further confirmation using multiple event histogram analysis of intracellular products by flow cytometry as commonly performed in studies of T cell differentiation.

An additional point emphasized by the present study is that macrophages have important homeostatic roles in addition to those of host defense. The essential function of macrophages in conduit artery remodeling in response to altered hemodynamic stresses is an example of the former (Bakker et al., 2008; Tang et al., 2008; Nuki et al., 2009). The inflammatory component of flow-mediated vascular remodeling is remarkably well orchestrated, such that adaptive changes in vessel size occur without apparent pathological sequelae. Different initiators of inflammation, namely tissue stress, tissue injury, and infection, elicit markedly different responses of homeostasis, tissue repair, and host defense, respectively. This suggests that different types of inflammation use distinct combinations of sensors, mediators, and effectors. It has been proposed that inflammation triggered by tissue stress be referred to as parainflammation to distinguish the process as an intermediate between the basal homeostatic state and classical inflammation triggered by pathogen-associated or damage-associated molecular patterns (Medzhitov, 2008). Because all forms of inflammation may have pathological consequences if unproductive and persistent, it is important to understand their underlying mechanisms. Indeed, it has been hypothesized that dysregulated parainflammation caused by tissue malfunction may underlie many chronic illnesses (Medzhitov, 2008). However, relatively little is known about inflammatory responses to tissue stress. We find that, unlike Gr1^{high} monocyte homing to the intima of atherosclerotic arteries known to be CXCR3 independent, Gr1^{low} macrophage accumulation and function in the adventitia of remodeling arteries is CXCR3 dependent.

MATERIALS AND METHODS

Clinical specimens. Blood, adventitia (stripped from the thoracic aorta), and/or common carotid arteries (midvessel and distal sinus) were obtained from five organ donors and adventitia was also obtained from three patients undergoing thoracic aortic aneurysm repair under protocols approved by the Yale University Human Investigation Committee, the West Haven VA Hospital, and the New England Organ Bank. Demographic and clinical information of the eight individuals included the following: mean age 42.1 ± 21.6 yr (range 5–67 yr); five males and three females; six Caucasians, one African-American, and one Hispanic; and four normal aortas, one atherosclerotic aorta, and three ascending aortic aneurysms.

Mice. C57BL/6, IL-1R$^{-/-}$, IL-6$^{-/-}$, iNOS$^{-/-}$, TNFR1$^{-/-}$, TNFR2$^{-/-}$, and RAG1$^{-/-}$ mice were purchased from The Jackson Laboratory. CXCR3$^{-/-}$ mice were obtained from C. Gerard (Harvard University, Cambridge, MA) and have been previously described (Hancock et al., 2000). All strains had been back bred to a C57BL/6 background for >10 generations. Procedures were performed in 8–12-wk-old male mice.

Carotid artery procedures. Animal studies were approved by the Yale University Institutional Animal Care and Use Committee. After anesthesia, a midline cervical incision was performed, the left external carotid artery was isolated and ligated with 6–0 silk, and the wound was closed with 5–0 prolene. After 6 h–10 d, RNA, protein, and cellular studies of the common carotid arteries were performed after saline perfusion of the vasculature. After 2 wk, morphometry studies of the common carotid arteries were performed after fixation-perfusion with 4% paraformaldehyde in PBS at a mean pressure of 100 mmHg, and then arteries were embedded in OCT medium. Alternatively, the tissues around the common carotid arteries of RAG1$^{-/-}$ mice were infiltrated with 30 µl nonpyrogenic saline or mouse IP-10 at 300 ng/µl (PeproTech) and the vessels were procured after 3 d for immunohistochemical analysis.

Morphometry. Hematoxylin and eosin–stained sections of the mid-common carotid arteries were analyzed by microscopy. Internal and external elastic lamina perimeters, as well as medial thickness at four quadrants, were measured and averaged over 10 separate sections using an image software program (ImageJ; National Institutes of Health).

Immunohistochemistry. Primary antibodies included rat anti–mouse CXCR3 (R&D Systems), rat anti–mouse F4/80 (Abcam), and rabbit anti–mouse IP-10 (AbD Serotec). Isotype-matched nonbinding immunoglobulin was used as negative control. Binding of secondary antibodies (Jackson ImmunoResearch Laboratories) was detected with Vectastain ABC reagent and AEC peroxidase substrate kits (Vector Laboratories). Sections were counterstained with hematoxylin (Sigma-Aldrich). Nuclei surrounded by positive immunostaining were enumerated at high magnification.

Immunofluorescence analysis. Primary antibodies for tissue sections included FITC-conjugated rat anti–mouse F4/80 (eBioscience), rabbit anti–mouse CXCR3 (MLB International), rabbit anti–mouse MMP2 (Millipore), goat anti–mouse MMP9 (R&D Systems), and goat anti–human FXIIIA (sc-18013, cross-reactive with mouse FXIIIA; Santa Cruz Biotechnology, Inc.). For analysis of human arteries, rabbit anti–human CD68 (Santa Cruz Biotechnology, Inc.) and mouse anti–human CXCR3 (BD) were used. Primary antibodies for cytospin preparations included rabbit anti–mouse MMP9 (Abnova) and goat anti–human FXIIIA. Isotype-matched nonbinding immunoglobulin was used as negative control. Detection of nonconjugated primary antibodies was visualized with secondary antibodies conjugated with FITC, TRITC (Jackson ImmunoResearch Laboratories), PE (Invitrogen), Alexa Fluor 594, or Alexa Fluor 488 (Invitrogen). Sections were counterstained with DAPI (Invitrogen).

Monocyte and macrophage isolation. Blood, single cell suspensions from minced spleens, and bone marrow cells from bilateral femurs and tibias were collected from 4–20 mice, red blood cells were lysed with ACK buffer (Bio Whittaker), and mononuclear cells were enriched by Lymphocyte Separation Medium (MP Biomedicals). For phenotyping experiments and adoptive transfer experiments with circulating cells, CD11b^{+} monocytes were positively isolated with antibody-coated magnetic beads and MACS LS cell separation columns (Miltenyi Biotec). Alternatively, for adoptive transfer experiments with bone marrow cells, CD11b^{+} myeloid cells were negatively selected by incubation with magnetic beads coated with antibodies to CD90 (T cell marker), B220 (B cell marker), DX5 (natural killer cell marker), and TER-119 (red blood cell marker), passage through MACS LS cell separation columns, and collection of the filtrate. 10^6 blood monocytes or 2.7×10^6 bone marrow myeloid cells were injected i.v. 12 h before left external carotid artery ligation.

For experiments with in vitro differentiated macrophages, unselected bone marrow cells were cultured in DME containing 10% FBS, 10% L929 cell–conditioned medium (enriched for M-CSF), 2 mM L-glutamine, 100 units/ml penicillin, and 100 µg/ml streptomycin (Invitrogen). Adherent cells were harvested after 7–10 d with a rubber scraper, resuspended in M-CSF–enriched and complete DME medium and treated with IP-10, LPS, and/or IL-4. FXIIIA-depleted FBS was used for analyses of FXIIIA protein expression and transglutaminase activity.

For isolation of artery-associated macrophages, common carotid arteries were pooled from 18–22 mice and digested with 125 U/ml collagenase XI, 60 U/ml hyaluronidase I, 60 U/ml DNase 1, and 450 U/ml collagenase I (Sigma-Aldrich) in phosphate-buffered saline containing 20 mM Hepes at 37°C for 1–2 h. The tissue pieces and supernatant were resuspended in RPMI-1640 medium at 4°C and sequentially passed through 0.5- and 0.1-mm sieves. Macrophages were isolated with CD11b antibody-coated magnetic beads and cell separation columns, and the selected cells were >95% CD11b^{+}. In certain experiments, the cells were further selected by flow cytometric sorting as indicated. For isolation of human macrophages, similar techniques were used as for mouse cells, except that enzymatic digestion of the aortic adventitia was for 2–4 h.

Quantitative PCR. Total RNA was isolated and DNase treated using the NanoPrep system (Agilent Technologies). Bulk reverse transcription was performed using random hexamer primers according to the MultiScribe RT system protocol (Applied Biosystems). Real-time RT-PCR reactions were performed in duplicate using Taqman PCR reagents and Taqman gene expression probes for GAPDH, IP-10, Mig, TNF, iNOS, F4/80, CXCR3, MMP2, MMP9, FXIIIA, Arginase I, Ym1, Fizz1, IL-10, and TGM2 (Applied Biosystems). DNase-treated RNA samples produced without RT enzyme served as negative controls. An iCycler and its system interface software (Bio-Rad Laboratories) were used to analyze the samples and data. Transcript expression levels were normalized to GAPDH.

Cytospins. Artery-associated macrophages were either immediately collected or treated with PMA at 500 ng/ml and ionomycin at 50 ng/ml (Sigma-Aldrich) in the presence of brefeldin A (BD) for 5 h. The cells were pelleted onto slides at 800 rpm for 10 min, air dried for 30 min, and fixed with 4% paraformaldehyde for 20 min. Before immunostaining, the cells were permeabilized with 0.1% Triton X-100 for 30 min and then blocked with 2% BSA for 1 h. The labeled slides were examined by fluorescence microscopy and the signal was quantified within the outline of individual cells as the percentage of area using image analysis software (ImageJ). Cells were considered positive for FXIIIA or MMP9 expression if FITC or TRITC signal exceeded 5% of cell area, respectively, and were classified as null, predominantly FXIIIA, predominantly MMP9, or dual expressors.

Western blotting. Cell lysates were prepared in RIPA buffer and boiled in SDS sample buffer for 10 min. An equal volume of samples was loaded, and proteins were separated by SDS-PAGE, transferred electrophoretically to a nitrocellulose membrane (Bio-Rad Laboratories), and blotted with goat

anti–human FXIIIA (Santa Cruz Biotechnology, Inc.), followed by horseradish peroxidase-conjugated secondary antibodies. Bound antibody was detected with Femto Maximum Sensitivity Substrate (Thermo Fisher Scientific).

Flow Cytometry. CD11b immunomagnetic bead-selected mouse cells were labeled with PerCP-CD11b, APC-CD42d, PE-Cy7-CD45.1, APC-CD45.2, FITC-F4/80 (eBioscience), APC-Gr1, APC-Ly-6C, V450-Ly-6G (BD), and PE-CXCR3 (R&D Systems) antibodies or isotype-matched irrelevant IgG. Similarly, CD11b-selected human cells were labeled with PE-Cy7-CD3, FITC-CD19, APC-CD56 (eBioscience), Pacific blue–CD14, FITC-CD16, PE-CXCR3 (BD), PE-CD15 (Beckman Coulter), APC-CD163 (R&D Systems), and APC-CD177 (Abcam) antibodies or isotype-matched irrelevant IgG. The labeled cells were analyzed using an LSR II flow cytometer (BD) and data were analyzed using FlowJo 6.3 (Tree Star, Inc.). CD11b-selected cells were also labeled with FITC-F4/80 and PE-CXCR3 antibodies and sorted using a FACSAria flow cytometer (BD) into $F4/80^+/CXCR3^+$ and $F4/80^+/CXCR3^-$ cell populations to analyze further by quantitative PCR. Alternatively, CD11b-selected cells were labeled with FITC-CD3, FITC-B220, and FITC-CD11c antibodies and the population negative for these lymphoid and dendritic cell markers was collected for cytospin preparations and immunofluorescence imaging.

Enzyme activity assays. Protein extracts from common carotid arteries were purified with gelatin sepharose beads (GE Healthcare) and subjected to 8% SDS-PAGE containing 1 mg/ml gelatin. Standards included purified MMP2 and MMP-9 (Millipore). After electrophoresis, the gels were washed and incubated overnight at 37°C in 100 mM NaCl, 2.5% Triton X-100, and 10 mM $CaCl_2$ and subsequently stained with Coomassie blue (Bio-Rad Laboratories). Zones of proteolysis appeared as clear bands against a blue background. For in situ gelatin zymography, OCT-embedded common carotid artery sections were incubated in DQ-gelatin solution (Invitrogen) for 2 h at 37°C, washed in PBS, and DAPI mounting mixture (Invitrogen) was applied to stain nuclei. For transglutaminase activity in intact arteries, tissue sections were incubated with biotinylated cadaverine (Invitrogen) at 5 mM for 90 min, washed, incubated with a 1:50 dilution of stock fluorescein (DTAF)-conjugated streptavidin (Jackson ImmunoResearch Laboratories) for 30 min in the dark, washed, and then visualized after application of DAPI mounting mixture. For transglutaminase activity in tissue and cell lysates, the samples were preincubated with α-thrombin (Haematologic Technologies) at 5 U/ml for 30 min, and enzyme activity was then measured based on the catalysis of covalent bonds between plate-bound poly-L-lysine residues and γ-carboxamide groups of soluble biotin-TVQQEL-OH substrate, according to the manufacturer's instructions (Sigma-Aldrich).

Statistical analysis. Paired Student's *t* test was used to compare two groups within the same animals (i.e., left vs. right arteries). An unpaired Student's *t* test was used to compare two groups between different animals (i.e., WT vs. $CXCR3^{-/-}$). One-way analysis of variance was used to compare between multiple groups. Statistical analyzes were performed using Prism 4.0 (GraphPad Software, Inc.). Differences with p-values <0.05 were considered to indicate statistical significance.

Online supplemental material. Fig. S1 shows successful adoptive transfer of WT bone marrow myeloid cells to WT and $CXCR3^{-/-}$ hosts. Fig. S2 shows that negatively selected bone marrow myeloid cells for adoptive transfer experiments are highly enriched for monocytes. Fig. S3 shows the expression of monocyte, but not granulocyte markers, by the selected population of circulating cells. Fig. S4 shows the overlapping expression patterns of small and large artery-infiltrating macrophages. Fig. S5 shows that IP-10 induces FXIIIA expression in isolated blood monocytes. Fig. S6 shows that human perivascular macrophages do not express lymphocyte or granulocyte markers. Table S1 summarizes the production of macrophage mediators in response to different proinflammatory factors. Online supplemental material is available at http://www.jem.org/cgi/content/full/jem.20100098/DC1.

This work was supported by the National Institutes of Health (PO1 HL70295). P.C.Y. Tang was supported by a Vascular Research Postdoctoral Training Grant from the NIH (T32 HL07950).

The authors have no conflicting financial interests.

Submitted: 14 January 2010
Accepted: 2 August 2010

REFERENCES

Auffray, C., D. Fogg, M. Garfa, G. Elain, O. Join-Lambert, S. Kayal, S. Sarnacki, A. Cumano, G. Lauvau, and F. Geissmann. 2007. Monitoring of blood vessels and tissues by a population of monocytes with patrolling behavior. *Science*. 317:666–670. doi:10.1126/science.1142883

Bakker, E.N., A. Pistea, J.A. Spaan, T. Rolf, C.J. de Vries, N. van Rooijen, E. Candi, and E. VanBavel. 2006. Flow-dependent remodeling of small arteries in mice deficient for tissue-type transglutaminase: possible compensation by macrophage-derived factor XIII. *Circ. Res.* 99:86–92. doi:10.1161/01.RES.0000229657.83816.a7

Bakker, E.N., H.L. Matlung, P. Bonta, C.J. de Vries, N. van Rooijen, and E. Vanbavel. 2008. Blood flow-dependent arterial remodelling is facilitated by inflammation but directed by vascular tone. *Cardiovasc. Res.* 78:341–348. doi:10.1093/cvr/cvn050

Bassiouny, H.S., R.H. Song, X.F. Hong, A. Singh, H. Kocharyan, and S. Glagov. 1998. Flow regulation of 72-kD collagenase IV (MMP-2) after experimental arterial injury. *Circulation*. 98:157–163.

Baumbach, G.L., and D.D. Heistad. 1989. Remodeling of cerebral arterioles in chronic hypertension. *Hypertension*. 13:968–972.

Cho, H.J., P. Shashkin, C.A. Gleissner, D. Dunson, N. Jain, J.K. Lee, Y. Miller, and K. Ley. 2007. Induction of dendritic cell-like phenotype in macrophages during foam cell formation. *Physiol. Genomics*. 29:149–160.

Combadière, C., S. Potteaux, M. Rodero, T. Simon, A. Pezard, B. Esposito, R. Merval, A. Proudfoot, A. Tedgui, and Z. Mallat. 2008. Combined inhibition of CCL2, CX3CR1, and CCR5 abrogates Ly6C(hi) and Ly6C(lo) monocytosis and almost abolishes atherosclerosis in hypercholesterolemic mice. *Circulation*. 117:1649–1657. doi:10.1161/CIRCULATIONAHA.107.745091

Fleming, T.J., M.L. Fleming, and T.R. Malek. 1993. Selective expression of Ly-6G on myeloid lineage cells in mouse bone marrow. RB6-8C5 mAb to granulocyte-differentiation antigen (Gr-1) detects members of the Ly-6 family. *J. Immunol.* 151:2399–2408.

Galis, Z.S., C. Johnson, D. Godin, R. Magid, J.M. Shipley, R.M. Senior, and E. Ivan. 2002. Targeted disruption of the matrix metalloproteinase-9 gene impairs smooth muscle cell migration and geometrical arterial remodeling. *Circ. Res.* 91:852–859. doi:10.1161/01.RES.0000041036.86977.14

Galkina, E., A. Kadl, J. Sanders, D. Varughese, I.J. Sarembock, and K. Ley. 2006. Lymphocyte recruitment into the aortic wall before and during development of atherosclerosis is partially L-selectin dependent. *J. Exp. Med.* 203:1273–1282. doi:10.1084/jem.20052205

Geissmann, F., S. Jung, and D.R. Littman. 2003. Blood monocytes consist of two principal subsets with distinct migratory properties. *Immunity*. 19:71–82. doi:10.1016/S1074-7613(03)00174-2

Gleissner, C.A., I. Shaked, K.M. Little, and K. Ley. 2010. CXC chemokine ligand 4 induces a unique transcriptome in monocyte-derived macrophages. *J. Immunol.* 184:4810–4818. doi:10.4049/jimmunol.0901368

Gordon, S., and P.R. Taylor. 2005. Monocyte and macrophage heterogeneity. *Nat. Rev. Immunol.* 5:953–964. doi:10.1038/nri1733

Gratchev, A., J. Kzhyshkowska, J. Utikal, and S. Goerdt. 2005. Interleukin-4 and dexamethasone counterregulate extracellular matrix remodelling and phagocytosis in type-2 macrophages. *Scand. J. Immunol.* 61:10–17. doi:10.1111/j.0300-9475.2005.01524.x

Guzik, T.J., N.E. Hoch, K.A. Brown, L.A. McCann, A. Rahman, S. Dikalov, J. Goronzy, C. Weyand, and D.G. Harrison. 2007. Role of the T cell in the genesis of angiotensin II–induced hypertension and vascular dysfunction. *J. Exp. Med.* 204:2449–2460. doi:10.1084/jem.20070657

Hancock, W.W., B. Lu, W. Gao, V. Csizmadia, K. Faia, J.A. King, S.T. Smiley, M. Ling, N.P. Gerard, and C. Gerard. 2000. Requirement of

the chemokine receptor CXCR3 for acute allograft rejection. *J. Exp. Med.* 192:1515–1520. doi:10.1084/jem.192.10.1515

Heller, E.A., E. Liu, A.M. Tager, Q. Yuan, A.Y. Lin, N. Ahluwalia, K. Jones, S.L. Koehn, V.M. Lok, E. Aikawa, et al. 2006. Chemokine CXCL10 promotes atherogenesis by modulating the local balance of effector and regulatory T cells. *Circulation.* 113:2301–2312. doi:10.1161/CIRCULATIONAHA.105.605121

Hong, H., S. Aksenov, X. Guan, J.T. Fallon, D. Waters, and C. Chen. 2002. Remodeling of small intramyocardial coronary arteries distal to a severe epicardial coronary artery stenosis. *Arterioscler. Thromb. Vasc. Biol.* 22:2059–2065. doi:10.1161/01.ATV.0000041844.54849.7E

Janatpour, M.J., S. Hudak, M. Sathe, J.D. Sedgwick, and L.M. McEvoy. 2001. Tumor necrosis factor–dependent segmental control of MIG expression by high endothelial venules in inflamed lymph nodes regulates monocyte recruitment. *J. Exp. Med.* 194:1375–1384. doi:10.1084/jem.194.9.1375

Kamiya, A., and T. Togawa. 1980. Adaptive regulation of wall shear stress to flow change in the canine carotid artery. *Am. J. Physiol.* 239: H14–H21.

Katschke, K.J. Jr., J.B. Rottman, J.H. Ruth, S. Qin, L. Wu, G. LaRosa, P. Ponath, C.C. Park, R.M. Pope, and A.E. Koch. 2001. Differential expression of chemokine receptors on peripheral blood, synovial fluid, and synovial tissue monocytes/macrophages in rheumatoid arthritis. *Arthritis Rheum.* 44:1022–1032. doi:10.1002/1529-0131(200105)44:5<1022::AID-ANR181>3.0.CO;2-N

Kim, W.K., X. Alvarez, J. Fisher, B. Bronfin, S. Westmoreland, J. McLaurin, and K. Williams. 2006. CD163 identifies perivascular macrophages in normal and viral encephalitic brains and potential precursors to perivascular macrophages in blood. *Am. J. Pathol.* 168:822–834. doi:10.2353/ajpath.2006.050215

Koh, K.P., Y. Wang, T. Yi, S.L. Shiao, M.I. Lorber, W.C. Sessa, G. Tellides, and J.S. Pober. 2004. T cell-mediated vascular dysfunction of human allografts results from IFN-gamma dysregulation of NO synthase. *J. Clin. Invest.* 114:846–856.

Kohrgruber, N., M. Gröger, P. Meraner, E. Kriehuber, P. Petzelbauer, S. Brandt, G. Stingl, A. Rot, and D. Maurer. 2004. Plasmacytoid dendritic cell recruitment by immobilized CXCR3 ligands. *J. Immunol.* 173:6592–6602.

Korshunov, V.A., and B.C. Berk. 2003. Flow-induced vascular remodeling in the mouse: a model for carotid intima-media thickening. *Arterioscler. Thromb. Vasc. Biol.* 23:2185–2191. doi:10.1161/01.ATV.0000103120.06092.14

Langheinrich, A.C., M. Kampschulte, T. Buch, and R.M. Bohle. 2007. Vasa vasorum and atherosclerosis - Quid novi? *Thromb. Haemost.* 97: 873–879.

Langille, B.L. 1996. Arterial remodeling: relation to hemodynamics. *Can. J. Physiol. Pharmacol.* 74:834–841. doi:10.1139/cjpp-74-7-834

Langille, B.L., M.P. Bendeck, and F.W. Keeley. 1989. Adaptations of carotid arteries of young and mature rabbits to reduced carotid blood flow. *Am. J. Physiol.* 256:H931–H939.

le Noble, F., D. Moyon, L. Pardanaud, L. Yuan, V. Djonov, R. Matthijsen, C. Bréant, V. Fleury, and A. Eichmann. 2004. Flow regulates arterial-venous differentiation in the chick embryo yolk sac. *Development.* 131: 361–375. doi:10.1242/dev.00929

Lessner, S.M., H.L. Prado, E.K. Waller, and Z.S. Galis. 2002. Atherosclerotic lesions grow through recruitment and proliferation of circulating monocytes in a murine model. *Am. J. Pathol.* 160:2145–2155.

Liu, P., Y.R. Yu, J.A. Spencer, A.E. Johnson, C.T. Vallanat, A.M. Fong, C. Patterson, and D.D. Patel. 2008. CX3CR1 deficiency impairs dendritic cell accumulation in arterial intima and reduces atherosclerotic burden. *Arterioscler. Thromb. Vasc. Biol.* 28:243–250. doi:10.1161/ATVBAHA.107.158675

Luster, A.D., and P. Leder. 1993. IP-10, a -C-X-C- chemokine, elicits a potent thymus-dependent antitumor response in vivo. *J. Exp. Med.* 178:1057–1065. doi:10.1084/jem.178.3.1057

Luster, A.D., S.M. Greenberg, and P. Leder. 1995. The IP-10 chemokine binds to a specific cell surface heparan sulfate site shared with platelet factor 4 and inhibits endothelial cell proliferation. *J. Exp. Med.* 182:219–231. doi:10.1084/jem.182.1.219

Martinez, F.O., S. Gordon, M. Locati, and A. Mantovani. 2006. Transcriptional profiling of the human monocyte-to-macrophage differentiation and polarization: new molecules and patterns of gene expression. *J. Immunol.* 177:7303–7311.

Martinez, F.O., A. Sica, A. Mantovani, and M. Locati. 2008. Macrophage activation and polarization. *Front. Biosci.* 13:453–461. doi:10.2741/2692

Medzhitov, R. 2008. Origin and physiological roles of inflammation. *Nature.* 454:428–435. doi:10.1038/nature07201

Mosser, D.M., and J.P. Edwards. 2008. Exploring the full spectrum of macrophage activation. *Nat. Rev. Immunol.* 8:958–969. doi:10.1038/nri2448

Nahrendorf, M., F.K. Swirski, E. Aikawa, L. Stangenberg, T. Wurdinger, J.L. Figueiredo, P. Libby, R. Weissleder, and M.J. Pittet. 2007. The healing myocardium sequentially mobilizes two monocyte subsets with divergent and complementary functions. *J. Exp. Med.* 204:3037–3047. doi:10.1084/jem.20070885

Nair, M.G., D.W. Cochrane, and J.E. Allen. 2003. Macrophages in chronic type 2 inflammation have a novel phenotype characterized by the abundant expression of Ym1 and Fizz1 that can be partly replicated in vitro. *Immunol. Lett.* 85:173–180. doi:10.1016/S0165-2478(02)00225-0

Nuki, Y., M.M. Matsumoto, E. Tsang, W.L. Young, N. van Rooijen, C. Kurihara, and T. Hashimoto. 2009. Roles of macrophages in flow-induced outward vascular remodeling. *J. Cereb. Blood Flow Metab.* 29: 495–503. doi:10.1038/jcbfm.2008.136

Oppenheim, J.J., and D. Yang. 2005. Alarmins: chemotactic activators of immune responses. *Curr. Opin. Immunol.* 17:359–365. doi:10.1016/j.coi.2005.06.002

Ranjbaran, H., Y. Wang, T.D. Manes, A.O. Yakimov, S. Akhtar, M.S. Kluger, J.S. Pober, and G. Tellides. 2006. Heparin displaces interferon-gamma-inducible chemokines (IP-10, I-TAC, and Mig) sequestered in the vasculature and inhibits the transendothelial migration and arterial recruitment of T cells. *Circulation.* 114:1293–1300. doi:10.1161/CIRCULATIONAHA.106.631457

Rudic, R.D., E.G. Shesely, N. Maeda, O. Smithies, S.S. Segal, and W.C. Sessa. 1998. Direct evidence for the importance of endothelium-derived nitric oxide in vascular remodeling. *J. Clin. Invest.* 101:731–736. doi:10.1172/JCI1699

Rudic, R.D., M. Bucci, D. Fulton, S.S. Segal, and W.C. Sessa. 2000. Temporal events underlying arterial remodeling after chronic flow reduction in mice: correlation of structural changes with a deficit in basal nitric oxide synthesis. *Circ. Res.* 86:1160–1166.

Saederup, N., L. Chan, S.A. Lira, and I.F. Charo. 2008. Fractalkine deficiency markedly reduces macrophage accumulation and atherosclerotic lesion formation in CCR2-/- mice: evidence for independent chemokine functions in atherogenesis. *Circulation.* 117:1642–1648. doi:10.1161/CIRCULATIONAHA.107.743872

Schwarz, J.B., N. Langwieser, N.N. Langwieser, M.J. Bek, S. Seidl, H.H. Eckstein, B. Lu, A. Schömig, H. Pavenstädt, and D. Zohlnhöfer. 2009. Novel role of the CXC chemokine receptor 3 in inflammatory response to arterial injury: involvement of mTORC1. *Circ. Res.* 104:189–200. doi:10.1161/CIRCRESAHA.108.182683

Selzman, C.H., B.D. Shames, L.L. Reznikov, S.A. Miller, X. Meng, H.A. Barton, A. Werman, A.H. Harken, C.A. Dinarello, and A. Banerjee. 1999. Liposomal delivery of purified inhibitory-kappaBalpha inhibits tumor necrosis factor-alpha-induced human vascular smooth muscle proliferation. *Circ. Res.* 84:867–875.

Sunderkötter, C., T. Nikolic, M.J. Dillon, N. Van Rooijen, M. Stehling, D.A. Drevets, and P.J. Leenen. 2004. Subpopulations of mouse blood monocytes differ in maturation stage and inflammatory response. *J. Immunol.* 172:4410–4417.

Swirski, F.K., P. Libby, E. Aikawa, P. Alcaide, F.W. Luscinskas, R. Weissleder, and M.J. Pittet. 2007. Ly-6C^{hi} monocytes dominate hypercholesterolemia-associated monocytosis and give rise to macrophages in atheromata. *J. Clin. Invest.* 117:195–205. doi:10.1172/JCI29950

Swirski, F.K., M. Nahrendorf, M. Etzrodt, M. Wildgruber, V. Cortez-Retamozo, P. Panizzi, J.L. Figueiredo, R.H. Kohler, A. Chudnovskiy, P. Waterman, et al. 2009. Identification of splenic reservoir monocytes and their deployment to inflammatory sites. *Science.* 325:612–616. doi:10.1126/science.1175202

Tacke, F., D. Alvarez, T.J. Kaplan, C. Jakubzick, R. Spanbroek, J. Llodra, A. Garin, J. Liu, M. Mack, N. van Rooijen, et al. 2007. Monocyte subsets differentially employ CCR2, CCR5, and CX3CR1 to accumulate within atherosclerotic plaques. *J. Clin. Invest.* 117:185–194. doi:10.1172/JCI28549

Tang, P.C., L. Qin, J. Zielonka, J. Zhou, C. Matte-Martone, S. Bergaya, N. van Rooijen, W.D. Shlomchik, W. Min, W.C. Sessa, et al. 2008. MyD88-dependent, superoxide-initiated inflammation is necessary for flow-mediated inward remodeling of conduit arteries. *J. Exp. Med.* 205: 3159–3171. doi:10.1084/jem.20081298

Taub, D.D., A.R. Lloyd, K. Conlon, J.M. Wang, J.R. Ortaldo, A. Harada, K. Matsushima, D.J. Kelvin, and J.J. Oppenheim. 1993. Recombinant human interferon-inducible protein 10 is a chemoattractant for human monocytes and T lymphocytes and promotes T cell adhesion to endothelial cells. *J. Exp. Med.* 177:1809–1814. doi:10.1084/jem.177.6.1809

Taub, D.D., D.L. Longo, and W.J. Murphy. 1996. Human interferon-inducible protein-10 induces mononuclear cell infiltration in mice and promotes the migration of human T lymphocytes into the peripheral tissues and human peripheral blood lymphocytes-SCID mice. *Blood.* 87:1423–1431.

Töröcsik, D., H. Bárdos, L. Nagy, and R. Adány. 2005. Identification of factor XIII-A as a marker of alternative macrophage activation. *Cell. Mol. Life Sci.* 62:2132–2139. doi:10.1007/s00018-005-5242-9

van Wanrooij, E.J., H. Happé, A.D. Hauer, P. de Vos, T. Imanishi, H. Fujiwara, T.J. van Berkel, and J. Kuiper. 2005. HIV entry inhibitor TAK-779 attenuates atherogenesis in low-density lipoprotein receptor-deficient mice. *Arterioscler. Thromb. Vasc. Biol.* 25:2642–2647. doi:10.1161/01.ATV.0000192018.90021.c0

van Wanrooij, E.J., S.C. de Jager, T. van Es, P. de Vos, H.L. Birch, D.A. Owen, R.J. Watson, E.A. Biessen, G.A. Chapman, T.J. van Berkel, and J. Kuiper. 2008. CXCR3 antagonist NBI-74330 attenuates atherosclerotic plaque formation in LDL receptor-deficient mice. *Arterioscler. Thromb. Vasc. Biol.* 28:251–257. doi:10.1161/ATVBAHA.107.147827

Veillard, N.R., S. Steffens, G. Pelli, B. Lu, B.R. Kwak, C. Gerard, I.F. Charo, and F. Mach. 2005. Differential influence of chemokine receptors CCR2 and CXCR3 in development of atherosclerosis in vivo. *Circulation.* 112:870–878. doi:10.1161/CIRCULATIONAHA.104.520718

Waeckel, L., Z. Mallat, S. Potteaux, C. Combadière, M. Clergue, M. Duriez, L. Bao, C. Gerard, B.J. Rollins, A. Tedgui, et al. 2005. Impairment in postischemic neovascularization in mice lacking the CXC chemokine receptor 3. *Circ. Res.* 96:576–582. doi:10.1161/01.RES.0000159389.55544.20

Whiting, D., G. Hsieh, J.J. Yun, A. Banerji, W. Yao, M.C. Fishbein, J. Belperio, R.M. Strieter, B. Bonavida, and A. Ardehali. 2004. Chemokine monokine induced by IFN-gamma/CXC chemokine ligand 9 stimulates T lymphocyte proliferation and effector cytokine production. *J. Immunol.* 172:7417–7424.

Zaba, L.C., J. Fuentes-Duculan, R.M. Steinman, J.G. Krueger, and M.A. Lowes. 2007. Normal human dermis contains distinct populations of CD11c+BDCA-1+ dendritic cells and CD163+FXIIIA+ macrophages. *J. Clin. Invest.* 117:2517–2525. doi:10.1172/JCI32282

Zhou, Y., T. Kurihara, R.P. Ryseck, Y. Yang, C. Ryan, J. Loy, G. Warr, and R. Bravo. 1998. Impaired macrophage function and enhanced T cell-dependent immune response in mice lacking CCR5, the mouse homologue of the major HIV-1 coreceptor. *J. Immunol.* 160:4018–4025.